



## Green synthesis and Characterization of Zinc Oxide Nanoparticles and Study Their Protective Effects Against Renal Failure in Male Rats

Hayder Hussein Abbas<sup>1\*</sup>, Narjis Hadi AL-Saadi<sup>2</sup>, Ayyed Hameed Hassan<sup>3</sup>

<sup>1,2</sup>Department of Chemistry, College of Sciences, University of Kerbala, Kerbala 56001, Iraq.

<sup>3</sup>College of Dentistry, University of Kerbala, Kerbala 56001, Iraq.

\*Corresponding author: Hayder Hussein Abbas, Department of Chemistry, College of Sciences, University of Kerbala, Kerbala 56001, Iraq, Email: hayder.h@s.uokerbala.edu.iq

Submitted: 14 January 2023; Accepted: 10 February 2023; Published: 12 March 2023

### ABSTRACT

Zinc oxide nanoparticles have been widely studied in recent decades due to their nano-medicine applications based on the physiological and biochemical agents that are often added as a food supplement in animal diets. This study aimed to synthesize, and characterization of zinc oxide nanoparticles using crude extract of *Ziziphus-Spina Christi* leaves and then investigated its protective effects against renal failure induced by adenine in male rats. Thirty-six male rats were randomly assigned to one of six groups and given adenine (100 mg/kg.BW) daily for thirty days. At the end of 30 days, blood and tissue samples were collected to evaluate kidney functions, antioxidant status, and histological changes. The UV-visible spectrum showed a strong absorption peak at 362 nm, which is specific to ZnO-NPs. Absorption peaks (400 and 500 cm<sup>-1</sup>) returned to Zn-O bonding in FT-IR spectroscopic investigation. X-ray diffraction (XRD) results showed the hexagonal wurtzite phase with an average crystal size calculated at 38.177 nm. Transmission electron microscopy (TEM) showed that particles had a spherical shape and measured an average diameter of 43.35 nm. In lowest doses, ZnO-NPs and *Ziziphus-Spina Christi* leaves extract effectively reduced the rise in kidney function parameters and improved biochemical changes suggestive of renal failure (Creatinine, urea, uric acid). Furthermore, total antioxidant capacity (TAC) and catalase levels were both increased while malondialdehyde (MDA) was dramatically decreased (CAT). In conclusion, the protective effects of ZnO-NPs and plant extract on ameliorating biochemical alterations were validated by histological tests.

**Keywords:** *Zinc oxide nanoparticles, Ziziphus-Spina Christi, Renal failure, Antioxidants*

### INTRODUCTION

Nanoparticles have different applications because they are reliable to provide a broad range of unusual uses and improved technologies for multiple applications such as industry, environment, medicine, and communications (1). Nanoparticles are comparable to naturally occurring proteins and

molecules in the human cell (2), this great interest is due to their small size and large surface area to volume ratio. The biological activity of nanoparticles increases as the total surface area of the particles increased (3), which gives rise to some of the superior properties of their bulk phase such as antimicrobial, catalytic, electronic, magnetic, and optical properties (4).

As a compound semiconductor with a large bandgap energy ( $E_g = 3.37$  eV) and large exciton binding energy (60 meV) at room temperature (5), ZnO-nanoparticles have found widespread use in recent years. This is due to the fact that ZnO is an ionic semiconductor with a large exciton binding energy, which makes it a good UV absorber (6). Several researchers have given serious consideration to the biological synthesis of ZnO-NPs using plant extracts due to the benefits it offers: it is safe for the environment, inexpensive, produces no hazardous byproducts, and can provide a usable yield quickly (7). The biomolecule components in the plant extract serve as reducing agents in redox processes, transferring electrons to zinc ions to create stable zinc oxide nanoparticles of controlled size and shape, increasing the manufacturing yield. Moreover, these chemicals serve as a capping agent, stopping particles from clustering together (8). As a food additive, zinc oxide nanoparticles (ZnO-NPs) may have effects linked to particle size and dose, facilitating zinc absorption (9). Moreover, the FDA has classified ZnO as GRAS (generally recognized as safe) (10). Damage to the kidneys lowers the quality of metabolic processes, immunological responses, detoxication, and antimicrobial defense, among other functions. Human kidneys play an important role in the filtration and concentration of numerous chemical substances that, in high enough concentrations, might be hazardous (11). Due to the pathologically lethal hormonal and metabolic disturbances, chronic renal failure (CRF) is considered a medical emergency. Nevertheless, when estimating the pathogenic damage of organs, certain animal models of chronic renal failure are utilized (12). So, the purpose of this work was to calculate the degree to which ZnO-NPs protect against adenine-induced chronic renal failure in male rats.

## MATERIALS AND METHOD

### *Chemical and Kits*

Zinc nitrate hexahydrate ( $Zn(NO_3)_2 \cdot 6H_2O$ , 99.0%) was purchased from CDH Co. (India), adenine with high purity grade, CAS NO.: 73-24-5 was supplied from Solarbio Co. (China), dimethyl sulfoxide (DMSO) with purity 99.9%

Min was obtained from Xi'an Sheerherb Biological Technology Co. (China). Kits for uric acid, creatinine, and urea were obtained from Solarbio Co. (China). Kits for total antioxidant capacity (TAC), catalase (CAT) kit, and malondialdehyde (MDA) content assay also were obtained from Solarbio Co. (China). Ethanol was supplied by Fluka Co. (Switzerland) with an assay of ~ 96%(v/v), and sodium hydroxide (NaOH) was purchased from BDH Co. (U.K.) with an assay of 99%.

### *Collection of plants*

Fresh *Ziziphus-Spina Christi* leaves were collected from the campus University of Kufa-College of Medicine. The fresh leaves were thoroughly washed under tap water to remove the adhered and then rinsed with distilled and de-ionized water to remove dust and other particles. The washed plant part was dried by exposing it to the sun through a window to protect it from direct sunlight. Then the dried leaves were sliced into small pieces and crushed using a mortar and pestle.

### *Preparation of Z.-spina Christi leaves extract*

Ten grams of crushed *Z.-spina Christi* leaves were dissolved in 100 ml de-ionized water in conical flasks and stirred it using a heating stirrer at 45°C for 15 minutes and then filtered through muslin cloth and centrifuged at 1500 rpm for 10 minutes. Then the crude extract was dried in air oven for 30 minutes at 90°C to obtain a powder.

### *Biosynthesis and purification of zinc oxide nanoparticles*

A one millimolar (1mM) stock solution of zinc nitrate hexahydrate was prepared by weighing out 0.0297 gm of zinc nitrate hexahydrate and dissolving in 100 ml deionized water. To synthesis of ZnO- nanoparticles adding 10 ml of *Z.-Spina Christi* leaves extract to 90 ml of 1 mM  $Zn(NO_3)_2 \cdot 6H_2O$  at room temperature. Freshly prepared 0.5 M of sodium hydroxide (NaOH) was added dropwise to the solution while being gently stirred to adjust the pH at 9. The mixture was heated on the magnetic stirrer for 2 hours at

60 °C until it transformed into the brownish-colored pellet. After that the mixture was cooled and centrifugated at 5000 rpm to purify the obtained pellet because it contains impurities on the surface of particles, and then washing with ethanol followed by de-ionized water several times to eliminate the water-soluble substances and any contaminants otherwise organic materials present on the surface of synthesized nanoparticles. The pure pellet was desiccated in a warm air oven at the temperature of 100°C for 90 minutes followed by the calcination step at 300 °C for 1 hr., that is important to forming ZnO-NPs. The calcinated ZnO-NPs were ready for characterization and subsequent applications.

#### **Optimization of the ZnO-NPs biosynthesis**

The reaction parameters, including plant extract volume, temperature, heating duration, pH, and Zn concentration, may be adjusted to control ZnO NPs synthesis. Hence, the biosynthesis process must be optimized to obtain the controllable size and production rate of ZnO NPs. In the interest of generating ZnO-NPs with a spherical form, smaller particles size, stability, and high yield, the optimization procedure in this work was conducted by modifying two experimental parameters, involving pH and reaction temperature.

#### **Effect of pH**

pH of the reaction mixture determines the types of ZnO-NPs formed, the different pH values (pH 5, 6, 7, 8, 9 and 10) were maintained using 0.5 M NaOH. The reaction time, reaction mixture concentration, and reaction temperature were kept constant.

#### **Effect of reaction temperature**

Temperature has been an important role in all reactions. The different temperature ranging from 40°C to 70°C at intervals of 10°C were maintained. The temperature was carried out using UV- visible spectrophotometer, and the absorbance of the solution was determined.

#### **Characterization of zinc oxide nanoparticles**

Zinc oxide nanoparticles were characterized using different modern techniques including the following:

##### **1- UV-Visible Spectroscopy**

The optical properties of ZnO-NPs were evaluated using UV–vis spectrophotometer (UV-1650PC, SHIMADZU, Japan). The spectra were set in between the wavelength of 300–700 nm range. In spectrophotometer de-ionized water was set as available reference and 4 ml solution of ZnO-NPs were subjected.

##### **2- Fourier transform infrared FT-IR spectroscopy**

FT-IR spectroscopy was used to determine the various functional groups involved in Z.-Spina Christi leaves extract and synthesized ZnO-NPs. These were recorded and compared using (IRPrestige-21, SHIMADZU, Japan) under the spectral range of (4000–400) cm<sup>-1</sup>. Identification of functional groups presented in the sample were recorded at room temperature, the dried extract and synthesized ZnO-NPs were carried out by the KBr pellet method. The presence of the various vibrational modes in aqueous extract and synthesized ZnO-NPs were investigated.

##### **3- X-ray diffraction (XRD)**

To determine the average crystalline size of biosynthesized ZnO-NPs and identification its crystalline features were characterized by XRD technique using (XRD-600, SHIMADZU, Japan) with Cu K $\alpha$  radiation (Voltage = 40 kV, Current =30 mA,  $\lambda$ =1.5406 Å, scan rate of 5.0o min<sup>-1</sup> and scan range of 2 $\theta$  from 20 – 80o). From the XRD data obtained, the crystalline size of the synthesized ZnO-NPs was calculated according to Debye–Scherrer’s equation (13).

$$D = \frac{k\lambda}{\beta \cos \theta}$$

Where, D is the average crystalline size,  $\lambda$  is the wavelength of X-ray (1.5406 Å),  $\theta$  is the Bragg’s diffraction angle,  $\beta$  is the XRD peak full width at

half maximum (FWHM) of the peak in radians, and  $k$  is the shape factor or Scherer's constant (0.98).

#### **4- Transmission Electron Microscopy (TEM)**

Transmission electron microscopy (TEM) is a microscopy technique whereby a beam of electrons is transmitted through an ultra-thin sample and interacting with it to form image involved information about the structure, crystallization, morphology and stress of a substance. TEM images for synthesized ZnO-NPs were investigated using a (JEOL JEM-1200 EX, Japan) transmission electron microscope operating at 100 kV. For TEM characterization, the ultrasound bath was used to diffuse a small amount of ZnO NPs into ethanol. The size and morphology of ZnO-NPs was investigated by suspending 0.01 g of the ZnO-NPs in 100 mL 95% ethanol and sonicating the suspension for 20 min.

#### **Experimental animals**

The experiment was carried out at the laboratory animal facilities- College of Sciences-University of Kufa, which has capabilities for working with laboratory animals. Thirty-six adult male of the species *Rattus norvegicus* that were in good condition and weighed between 200 and 205 g each were unsealed. These rats were obtained from the animal house at the Faculty of Sciences -University of Kufa. Prior to their usage, rats were housed in an animal home for two weeks in order to acclimate them to the conditions of the laboratory. The research was conducted from the beginning of May through the middle of August 2022. These animals were housed in a controlled setting that maintained constant parameters of temperature (25-27 °C) and relative humidity (50-60 %). The animals were separated and put in a cage made of plastic with diameters of 50×35×15 cm (14).

#### **The Experimental Design**

Thirty-six male rats were used in this study and divided into six equal groups; each group consisted of 6 male rats as follows:

1-First group (G-I): Rats received of 0.5 ml DMSO (5% v/v) one time daily for 30 days.

2- Second group (G-II): Rats were gavaged 0.5 ml of adenine (100 mg/kg. BW) dissolved by DMSO one time daily for 30 days to induce renal failure. The dose of adenine was chosen from the previous study by (15) based on the original method by (16).

3-Third group (G-III): Rats were received 0.5 ml of ZnO-NPs (10 mg/kg B.W) one time daily for 30 days (17).

4-Fourth group (G-IV): Rats were received 0.5 ml of Z.-Spina Christi leaves extract (10 mg/kg B.W) one time daily for 30 days. The dose of Z.-Spina Christi leave extract according to (18).

5- Fifth group (G-V): Rats were co-administrated 0.25 ml of adenine (100 mg/kg.BW) and 0.25 ml of ZnO-NPs (10 mg/kg B.W) at the same time for 30 days (19).

6-Sixth group (G-VI): Rats were co-administrated 0.25 ml of adenine (100 mg/kg.BW) and 0.25 ml Z.-Spina Christi leaves extract (10 mg/kg B.W) at the same time for 30 days (20).

The rats were weighed and recorded the weights before the beginning of the treatment and weekly during the treatment period.

#### **Collection of blood**

##### **Blood Specimens**

After 30 days of experiment rats were anesthetized by placing them in a closed jar containing cotton rinsed with chloroform to be sedated for the next step, which is blood collection via cardiac puncture in sterile syringes by needle prick in the heart draining 5ml of blood carefully, then blood placed in a test tube containing gel which leaves for 30 minutes at room temperature, and then used for obtaining serum by centrifuging at 3000 for 15 minutes. The serum was then divided into 1.5 ml Eppendorf tubes and stored at (-20°C) for further examinations.

### ***Tissue Sampling***

After collecting blood and puncturing the heart, rats were killed by dislocating their necks. The kidney was then carefully isolated. Each animal's kidney tissue samples were weighed, washed with saline, fixed in 10% neutral formalin, and paraffin-embedded. Hematoxylin and eosin (H & E) were used to stain 5- $\mu$ m-thick sections for the histological evaluation. Using a light microscope (Olympus BH-2, Tokyo, Japan), histological changes in the rat kidney were evaluated.

### ***Biochemical analysis***

#### ***Evaluation of kidney function tests***

kidney function tests of rat serums (uric acid, urea, and creatinine) were spectrophotometrically determined according to special kits.

#### ***Assessments of antioxidants statues***

The antioxidants statues which included total antioxidant capacity (TAC), catalase (CAT) and oxidative stress parameters malondialdehyde (MDA) as a marker for lipid peroxidation, were analyzed spectrophotometrically in order using special diagnostic kits.

### ***Statistical Analysis***

One-way analysis of variance (ANOVA) and Tukey post hoc test were used to identify statistically significant differences between the means at the P 0.05 level, and the findings were reported as mean  $\pm$  standard deviation (SD) of the groups under study. Statistical Package for the Social Sciences was used for all analyses (Version 19, SPSS Inc., Chicago, IL, USA).

## **RESULTS**

### ***Biosynthesis of zinc Oxide Nanoparticles***

By using color changes, synthesis of ZnO-NPs can be detected. Furthermore, this change in color was observed after the 15 minutes when mixed of zinc nitrate hexahydrate salt solution with the aqueous extract of *Z.-spina Christi* leaves. The principal behind nanoparticles produce is Zinc nitrate hexahydrate reduced into ZnO-NPs and color of solution was changed from yellow into deep yellow and the intensity of color increased with the time until the solution change into the brownish colored pellet (Fig. 1-a), that indicated the point of metallic nanoparticles synthesis. nanoparticles synthesis process was detected by UV-visible spectroscopy. Finally, the pellet of ZnO NPs was dried at 300 °C for 1 hr after the completion of process yellowish-white color ZnO-NPs powder were obtained (fig.1-b).

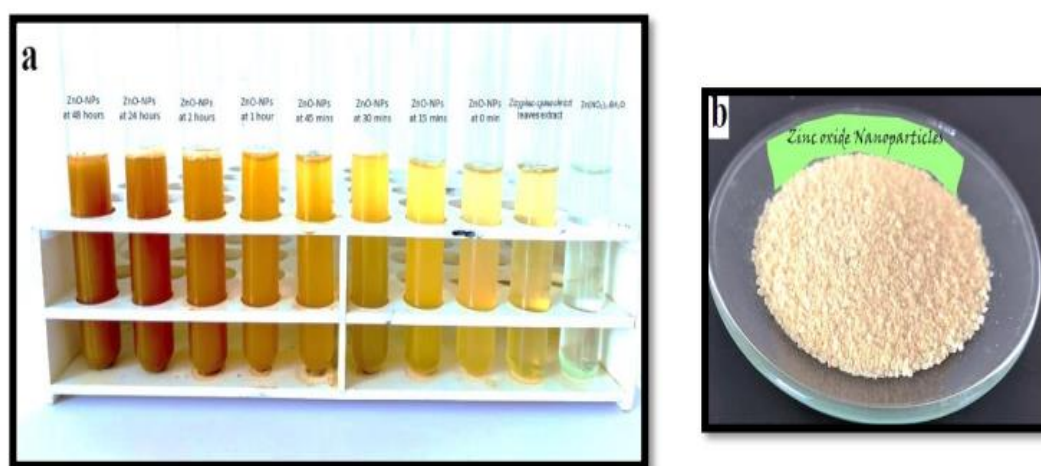


**FIGURE 1:** (a) The gradual change in the color of the synthesized ZnO-NPs from *Z.-spina Christi* leaves and zinc nitrate hexahydrate with time (0 min- 48 hours). (b) Yellowish-white powder of ZnO-NPs.

### Characterization of Zinc Oxide Nanoparticles Ultraviolet-Visible Spectroscopy (UV-Vis Spectroscopy)

The UV-vis absorbance spectra were obtained at room temperature in the range of 200-700 nm to explore the optical property of the biosynthesized ZnO-NPs (Fig. 2-a), where the significant absorption peak at 362 nm corresponds to the optical absorption of the ZnO-NPs produced.

The strength of the absorption peak enhanced as the duration of mixing *Z. spina Christi* leaves extract with an aqueous solution of Zn (NO<sub>3</sub>)<sub>2</sub>·6H<sub>2</sub>O increased. Even after 24 hours, the absorbance remained constant, showing that the reaction was complete and the ZnO-NPs generated were stable at room temperature without agglomeration (fig. 2-b).

The reaction temperature is critical in the synthesis of ZnO-NPs. The effect of varying temperatures on ZnO-NPs production is investigated at temperatures ranging from 40 to 70 degrees Celsius. As shown in figure 2.c, no characteristic absorption peaks were observed at lower temperatures of 40 and 50 degrees Celsius,

whereas characteristic absorption peaks were observed at higher temperatures (60 and 70 degrees Celsius). As compared to other temperatures, the maximum synthesis of ZnO-NPs was observed at 60°C, and a sharp peak was found by UV-vis spectrophotometer at 362 nm.

Synthesis of ZnO-NPs with respect to variation of solution pH from acidic to basic medium is shown in (fig. 2-d), absorbance of the synthesized ZnO-NPs was observed gradually (from pH 5 to pH 10). At a lower solution pH (pH 5 to pH 6), observed no characteristics absorption peak of ZnO-NPs. On the other hand, increasing pH to 7 with 0.5M NaOH, the absorption spectrum exhibits a shift to 340 nm indicating the production of ZnO-NPs. When pH of the reaction mixture is greater than pH 7, the absorbance of synthesized ZnO-NPs was increased from pH 8.0 to pH 9.0, while decreased between pH 9.0 and pH 10.0. The results showed at high solution pH (pH 9.0), the characteristic absorption peak of the synthesized ZnO-NPs observed at 362 nm (fig. 2-d).

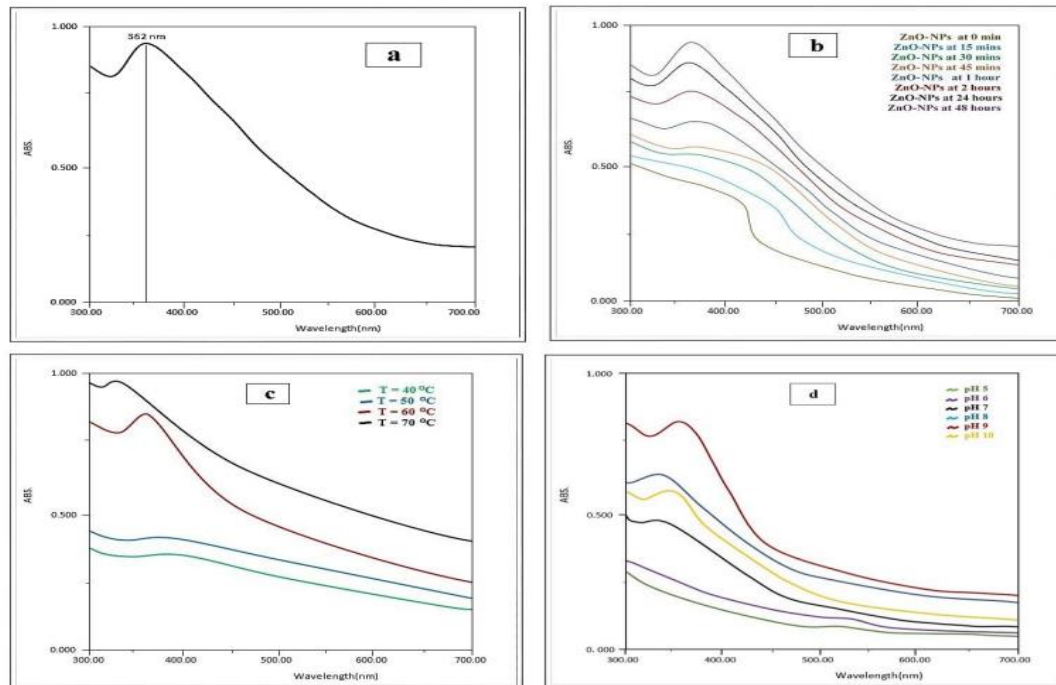


**FIGURE 2:** UV-Visible spectra: (a) for the ZnO-NPs synthesized at 362 nm. (b) At different time of incubation. (c) Effect the temperature on Zn-NPs synthesizes. (d) At different pH.

### Fourier Transform Infrared Spectroscopy (FT-IR)

Identifying and comparison of functional groups between synthesized ZnO-NPs using *Z. spina Christi* leaves extract and the *Z. spina Christi* leaves extract alone is shown in Figure 3. FT-IR spectrum of *Z. spina Christi* leaves extract alone (fig. 3-a) showed the broad band observed at 3377.36 cm<sup>-1</sup> corresponds to O-H stretching of phenolic and alcoholic compounds as well as carbohydrates (21). Besides, the peaks at 2917.94 cm<sup>-1</sup> to 2612.71 cm<sup>-1</sup> correspond to the symmetric and asymmetric stretching vibrations of C-H in -CH<sub>3</sub> and -CH<sub>2</sub>- of aliphatic hydrocarbons chains, 1648.58 cm<sup>-1</sup> (C=O stretching vibration) related to flavonoid and amino acids or carboxylic acid salt (COO<sup>-</sup>) (22). Moreover, 1572.48 cm<sup>-1</sup> (O-H bending vibrations), 1388.75 cm<sup>-1</sup> (C-O stretching of the ester group), 1255.66 cm<sup>-1</sup> (C-O asymmetric stretching in cyclic polyphenolic compounds), and 1058.92 cm<sup>-1</sup> to 619.18 cm<sup>-1</sup> indicating the

presence of (C-N stretch) aromatic amines and alkyl halides respectively (23). The vibrational bands above were mostly found in the *Z. spina Christi* leaves extract. These peaks were disappeared or shifted to lower frequency indicates the successful participation of phytochemicals compounds was presented in the *Z. spina Christi* leaves as reducing and stabilizing agents in the synthesis of ZnO-NPs (24), that facilitates the conversion of metal ions to metal-NPs. This is shown by the peak for the shifted carbonyl groups (C=O) at 1612.48 cm<sup>-1</sup>. The shifted peaks were, 3377.36 cm<sup>-1</sup> to 3415.83 cm<sup>-1</sup>, 2917.94 cm<sup>-1</sup> to 2911.76 cm<sup>-1</sup>, 1648.58 cm<sup>-1</sup> to 1612.48 cm<sup>-1</sup>, 1588.63 cm<sup>-1</sup> to 1496.69 cm<sup>-1</sup>, 1255.66 cm<sup>-1</sup> to 1202.14 cm<sup>-1</sup> and 1058.92 cm<sup>-1</sup> to 1031.92 cm<sup>-1</sup>. Furthermore, the significant vibration of stretching peaks appeared at 451.34 cm<sup>-1</sup>, 445.56 cm<sup>-1</sup> and 424.34 cm<sup>-1</sup> (fig. 3-b), corresponding to Zn-O vibrational stretching that further confirmed the formation of ZnO-NPs.

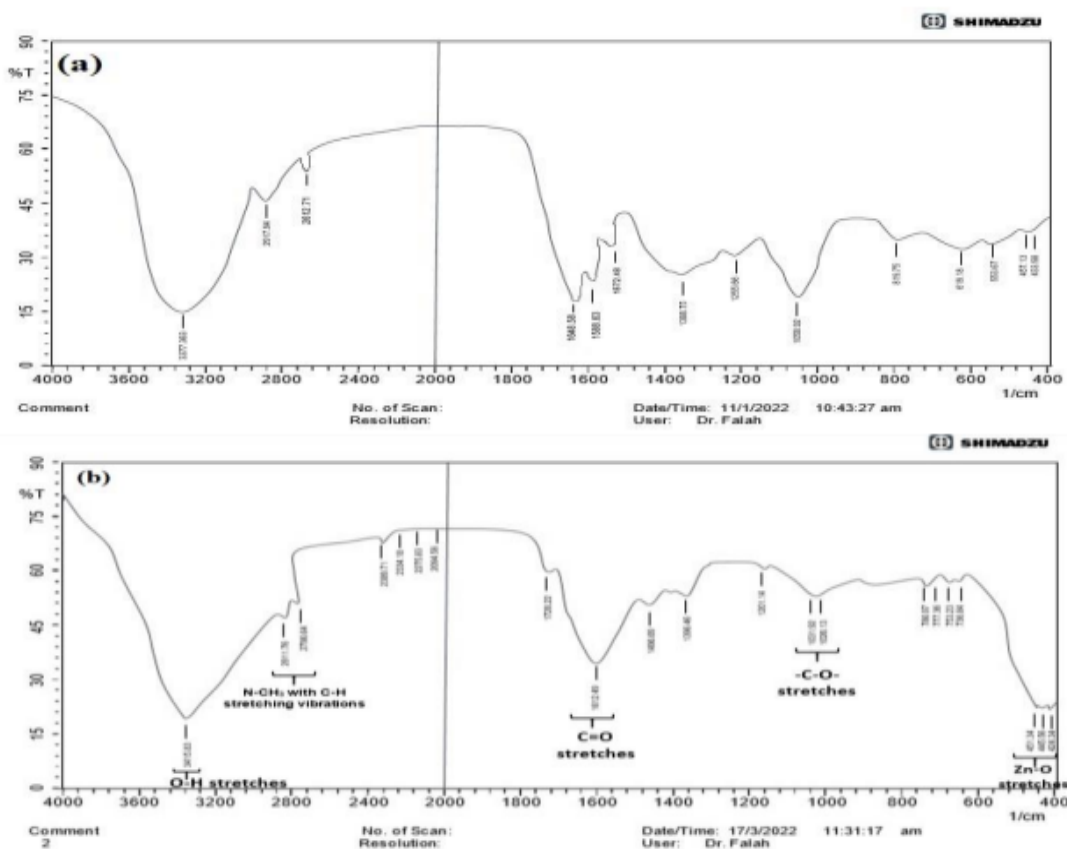


FIGURE 3: FT-IR spectrum, (a) *Z. spina Christi* leaves extract powder. (b) ZnO-NPs synthesized.

### ***X-ray Diffraction (XRD)***

The nanoparticles synthesized were studied and confirmed by using XRD technique to determine their phases, structures, and crystal orientations. The observed diffraction peaks of the biosynthesized ZnO-NPs in terms of intensities and positions were at  $2\theta$  31.77 $^\circ$  (100), 33.21 $^\circ$  (002), 36.59 $^\circ$  (101), 44.64 $^\circ$  (102), 48.74 $^\circ$  (110), 55.91 $^\circ$  (103), 63.27 $^\circ$  (200), 66.12 $^\circ$  (112), 69.09 $^\circ$  (201), 73.73 $^\circ$  (004), and 76.57 $^\circ$  (202) as

shown in figure 4 which strongly detected the hexagonal wurtzite structure of ZnO-NPs.

Based on the FWHM of most intense diffraction peaks table (1) (100%), (66%) and (41%) at  $2\theta$  with 36.59 $^\circ$  (101), 33.21 $^\circ$  (002), 31.77 $^\circ$  (100) respectively. Using Debye-Scherrer equation, average crystalline size was calculated to be 38.177 nm confirming the nano size for the synthesized ZnO-NPs.

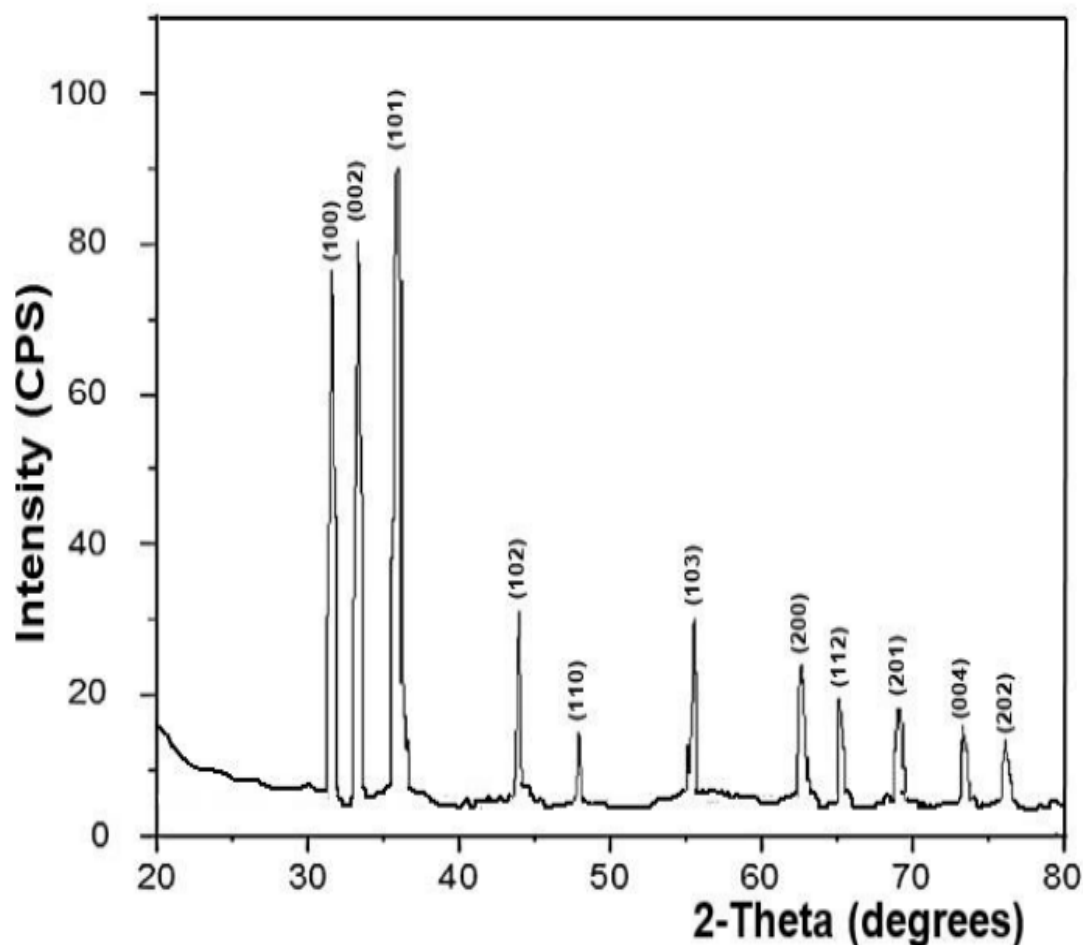


**FIGURE 4:** X-Ray diffraction (XRD) of synthesized ZnO-NPs from *Z.-spina Christi* leaves extract.

### ***Transmission Electron Microscopy (TEM)***

The size distribution and morphological characters of ZnO-NPs was observed under TEM analysis (Fig. 5-a, b) were uniform in size. Agglomeration was common, due to the ultra-small size and high surface energy of ZnO-NPs. Also, TEM micrographs showed most the ZnO-

NPs were presented in a spherical shape. The histogram of the size distribution of ZnO-NPs was generated in based on TEM data (fig. 5-c). The majority of ZnO NPs measured fell in the range of 35 - 50 nm in diameter with an average size of 43.35 nm in diameter.

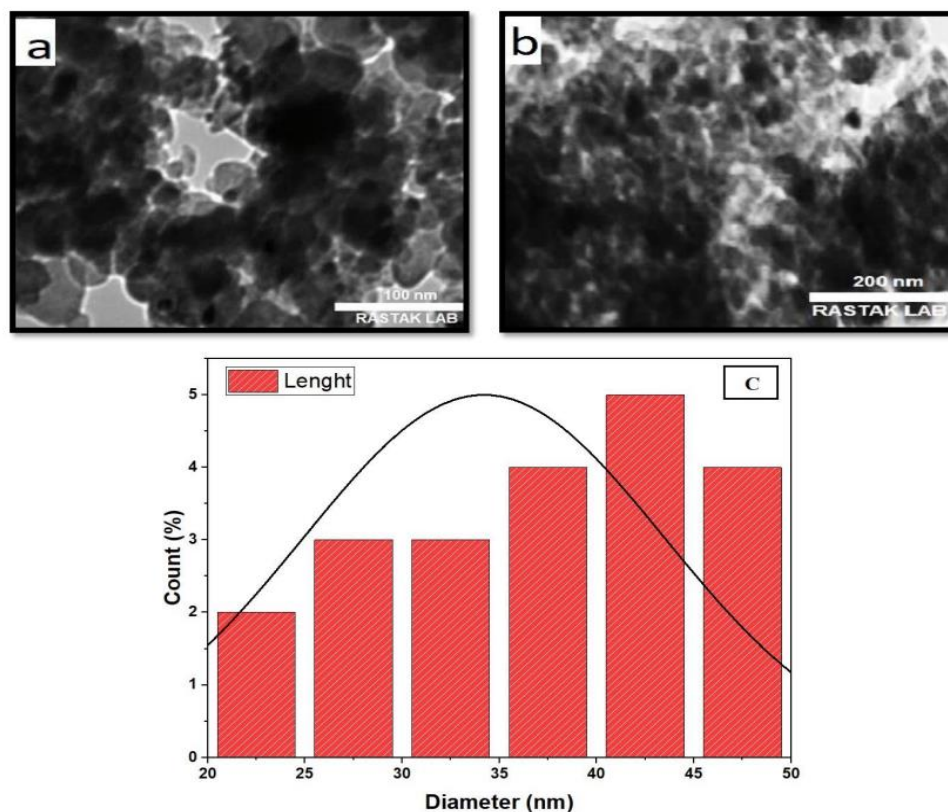


**FIGURE 5:** TEM micrograph of synthesized ZnO-NPs from *Z.-spina Christi* leaves extract. (a) Scale at 100 nm. (b) Scale at 200 nm. (c) The size distribution histogram of ZnO-NPs.

***Effects of ZnO-NPs and Z.-Spina Christi leaves extract on body weight and kidney biochemical parameters with renal failure induced by adenine***

In this study, healthy male rats treated with ZnO-NPs and aqueous extract of *Z.-Spina Christi* leaves for sequential 30 days displayed some important abnormal changes in the biochemical parameter levels. These parameters changes are slightly insignificant compared to those caused by disease induction "adenine-induced renal failure" and have not lived up enough to cause any detected histological changes in both kidney and liver tissue sections as showed during the normal renal architectures.

***1- Effect on Body weight changes***

The statistical analysis demonstrated the effect of ZnO-NPs on the bodies weight (gm) of male rats. As shown in table 1, control group rats were

grown during the experiment by about ( $10 \pm 2$  gm) after gavaged DMSO only. Adenine groups rats significantly decreased in body weight starting from the 2nd week of administration to the end of the 4th week in comparison to control group rats ( $P < 0.001$ ). The body weight of rats with oral administration of ZnO-NPs (10 mg/kg B.W) alone significantly decreased when compared to the control group ( $P < 0.05$ ), but their weights elevated when compared to the adenine group (Table1), while the body weights of rats treated with *Z.-Spina Christi* leaves extract (10 mg/kg B.W) slightly decreased ( $P = 0.04$ ) in comparison to the control group. Finally, body weights were a significantly increased ( $P < 0.02$ ) after co-administration of adenine plus ZnO-NPs (10 mg/kg B.W) or adenine plus *Z.-Spina Christi* leaves extract (10 mg/kg B.W) at the same time (G-V and G-VI) when compared to the adenine group, but their weights still lower by comparison to control group.

**TABLE 1:** Effect of ZnO-NPs and Z.-Spina Christi leaves extract on adenine-induced body weight changes.

Period time Groups	Day-0 Weight (gm)	Week-1 Weight (gm)	Week-2 Weight (gm)	Week-3 Weight (gm)	Week-4 Weight (gm)
G-I	204.19±0.32	206.98±0.35	209.74±1.29	212.16±0.96	215.85±0.48
G-II	204.23±0.05	197.52±0.06	193.03±0.26	187.54±0.73	182.38±1.13
G-III	204.27±0.06	205.14±0.46	207.65±0.57	209.85±0.59	211.50±0.67
G-1V	204.08±0.29	206.13±0.57	208.96±0.62	211.35±0.66	214.69±0.81
G-V	204.25±0.10	201.16±0.16	197.23±1.06	194.41±1.19	191.26±1.64
G-VI	204.36±0.43	203.26±0.64	199.51±0.91	196.84±0.38	194.35±0.59
Tukey Test	0.317	0.422	0.846	0.863	1.513

Notes: Values in the table are expressed as mean ± SD. n=6 male rats in each group, P ≤0.05 (One-Way ANOVA followed by Tukey post-hoc test). SD: Standard deviation.

G-I: Control group, G-II: Adenine group, G-III: ZnO-NPs, G1V: Z.-Spina Christi leaves extract group, G-V: Adenine + ZnO-NPs, G-VI: Adenine + Z.-Spina Christi leaves extract group.

**2- Effect on kidney function tests**

The results in table 2 showed the rats treated with adenine led a significant increase (P<0.001) in serum concentrations of uric acid, urea, and creatinine when compared to the control group. These parameters significantly reduced (P<0.05) after administration of rats with ZnO-NPs at a

dose (10 mg/kg B.W) (G-III) when compared to the adenine group, but not completely restored these changes as in the control group, also showed the slightly significant elevation (P< 0.05) in serum concentrations of uric acid, urea and creatinine in rats administered with Z.-Spina Christi leaves extract (G-IV). At the same table, results as showed in the both treatment groups (G-V and G-VI), co-administration of adenine plus ZnO-NPs (10 mg/kg B.W) or adenine plus Z.-Spina Christi leaves extract (10% w/v), resulted in a significant reduction (P< 0.05) in serum concentrations of uric acid, urea and creatinine in comparison to adenine group, but their values still elevated when comparing to control group (P< 0.03).

**TABLE 2:** Effect of ZnO-NPs and Z.-Spina Christi l. extract on kidney function Parameters in serum of rats within induced chronic renal failure

Parameters Groups	Uric acid mg/dl	Urea mg/dl	Creatinine mg/dl
G-I	1.24±0.08	13.66±1.10	0.26±0.03
G-II	3.22±0.19	105.88±1.96	0.84±0.05
G-III	1.68±0.10	16.07±2.20	0.31±0.04
G-1V	1.31±0.09	14.05±1.37	0.29±0.03
G-V	2.73±0.14	87.03±1.60	0.68±0.01
G-VI	2.48±0.15	73.41±0.93	0.51±0.01
Tukey Test	0.094	1.705	0.023

Notes: Values in the table are expressed as mean  $\pm$  SD. n=6 male rats in each group,  $P \leq 0.05$  (One-Way ANOVA followed by Tukey post-hoc test). SD: Standard deviation.

G-I: Control group, G-II: Adenine group, G-III: ZnO-NPs, G-IV: Z.-Spina Christi leaves extract group, G-V: Adenine + ZnO-NPs, G-VI: Adenine + Z.-Spina Christi leaves extract group.

### 3- Effect on antioxidants statuses

Results in table 3 showed the antioxidant levels, TAC, CAT, and MDA, where noticed that TAC and CAT levels were remarkably reduced while MDA concentration was significantly elevated after the male rats administrated with adenine (G-II) in comparison to the control group ( $P > 0.02$ ). Group rats after administration of ZnO-NPs (10 mg/kg B.W) significantly increased TAC and CAT levels when compared to the adenine group, but significantly less decreased in comparison to the

control group, while MDA concentration significantly reduced when compared to the adenine group, but still less high in comparison with the control group ( $P < 0.05$ ). Moreover, as shown in table 3, rats when administered of Z.-Spina Christi leaves extract (10 mg/kg B.W) revealed a slight difference in TAC, CAT and, MDA levels when compared to the control group ( $P < 0.05$ ). Finally, the co-administrated of adenine plus ZnO-NPs (10 mg/kg B.W) (G-V) or adenine plus Z.-Spina Christi leaves extract (10 mg/kg B.W) (G-VI) resulted in a significant increase in TAC and CAT levels compared to the adenine group ( $P < 0.05$ ), but still lower when comparison to the control group ( $P < 0.04$ ), this increase was accompanied with a significant reduction in MDA concentration when compared to adenine group ( $P < 0.05$ ), but was significantly increased when compared to the control group ( $P < 0.04$ ).

**TABLE 3:** The Effect of ZnO-NPs and Ziziphus-Spina Christi leaves extract on the antioxidant levels in serum of rats within chronic renal failure.

Parameters Groups	TAC ( $\mu\text{mol/ml}$ )	CAT U/ml	MDA ( $\mu\text{mol/ml}$ )
G-I	17.56 $\pm$ 0.80	10.83 $\pm$ 1.37	0.49 $\pm$ 0.02
G-II	6.84 $\pm$ 0.87	1.69 $\pm$ 0.03	4.16 $\pm$ 0.41
G-III	15.45 $\pm$ 0.17	9.15 $\pm$ 0.69	0.62 $\pm$ 0.10
G-IV	16.94 $\pm$ 0.84	10.13 $\pm$ 1.25	0.54 $\pm$ 0.06
G-V	9.71 $\pm$ 0.07	2.74 $\pm$ 0.25	3.53 $\pm$ 0.37
G-VI	13.52 $\pm$ 0.61	6.75 $\pm$ 0.33	2.29 $\pm$ 0.30
Tukey Test	0.642	0.917	0.238

Notes: Values in the table are expressed as mean  $\pm$  SD. n=6 male rats in each group. Means in the same column with different superscript letter(s) are significantly different,  $P \leq 0.05$  (one-way ANOVA followed by Tukey post-hoc test). SD: Standard deviation.

TAC = total anti-oxidant capacity, CAT = catalase, MDA= malonaldehyde.

G-I: Control group, G-II: Adenine group, G-III: ZnO-NPs, G-IV: Z.-Spina Christi leaves extract group, G-V: Adenine + ZnO-NPs, G-VI: Adenine + Z.-Spina Christi leaves extract group.

### 4- Histological Study

Figure 6 showed the results of a histological study of the kidney tissue from male rats for six groups after 30 days of dosage. The kidneys of control rats (G-I) showed no marker of damage, normal renal cortexes, normal renal architecture and, normal nephritic tubules (Fig. 6-K1). Histological markers of second group rats (G-II) with adenine-administered showed significant acute damage of the renal tissue. Their kidneys showed renal vein congestion and hypertrophy of renal glomeruli, besides necrosis and dilation of normal renal tubular (Fig. 6-K2). Third group rats

(G-III) that administrated with ZnO-NPs (10 mg/kg B.W) showed that slightly inflammatory around blood vessels, but no significant glomerular changes (Fig. 6-K3). Also, the rats in fourth group (G-IV) when administration of Z.-Spina Christi leaves extract (10 mg/kg B.W) showed the histological changes that involves: the normal structure of the renal cortex except the

less degradation of some renal tubules (Fig. 6-K4). The kidneys of both fifth and sixth groups rats when co-administration of adenine plus Z.-Spina Christi leaves extract (G-V) or adenine plus ZnO-NPs (10 mg/kg B.W) (G-VI) lead to a significantly lowered the markers and histological features were improved to normal when comparison with adenine group rats (Fig. 6-K5 and K6).

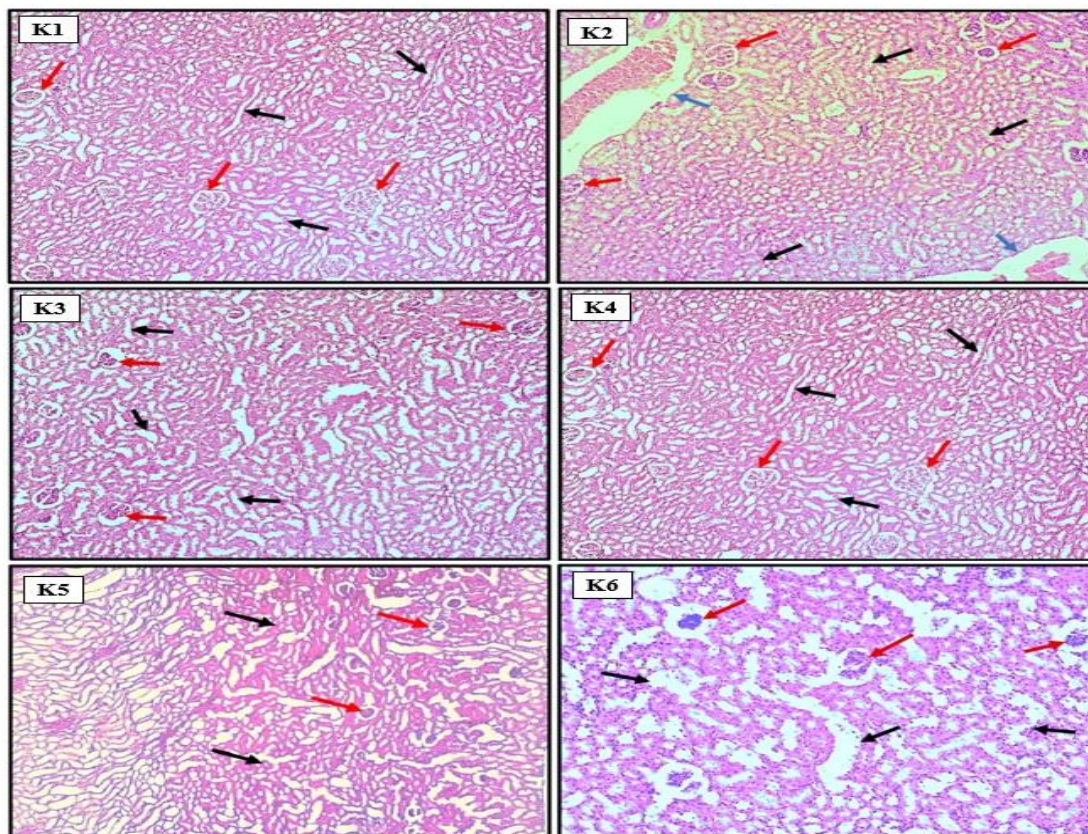


**FIGURE 6:** Effects of ZnO-NPs and Z.-Spina Christi leaves extract on the histological appearance of kidney tissues in male rats with chronic renal failure induced by adenine. The tissue is stained by H&E stain and the section is captured using light microscope and digital camera at 10X magnification scale. K1: Kidney of male rats in (control group) were treated with DMSO only that shows normal renal glomerulus (black arrows) and normal renal tubules (red arrows) without any significant occupied lesion. K2: Kidney of male rats were treated with (Adenine) shows acute renal glomerulus hypertrophy (Black arrows) with expansion in tubular lumen and the renal glomeruli show severe atrophied lesion in some area of section (Red arrows) and clear renal vein congestion (Blue arrow). K3: Kidney of male rats were treated with (ZnO-NPs 10 mg/kg.bw) shows normal renal glomerulus (Red arrows) except slight degeneration and cystic extended of normal renal tubules (Black arrow) without any significant occupied lesion (SOL). K4: Kidney of male rats were treated with (Z.-Spina Christi leaves extract (10 mg/kg B.W)) shows no significant change in renal glomerulus (Red arrows), but there very less narrowing in tubular lumen without any significant occupied lesion (Black arrows). K5: Kidney of male rats were treated with (Adenine + ZnO-NPs (10 mg/kg B.W)) shows renal glomerular hypertrophy (Red arrows) with very slight narrowing in tubular lumen (Black arrows). K6: Kidney of male rats were treated with (Adenine + Z.-Spina Christi leaves extract (10 mg/kg B.W)) shows renal tubular hypertrophy or many intact tubules

(Black arrows) with less narrowing in tubular lumen and the renal glomerular tuft show very mild atrophied lesion in some area of section (Red arrows) 20X.

## DISCUSSION

The synthesis of ZnO-NPs using biological techniques has received a lot of interest recently, mainly to its safety, eco-friendliness, and low cost, in addition to the removal of high energy or harmful chemical by-products utilized in chemical methods (25). Moreover, phytochemicals included in plant extracts have an important function in reducing, capping, and stabilizing nanoparticles. The flavonoids found in *Z.-spina Christi* leaves are important reductants of metal precursor salts.

Several scientists shown that reaction time is an important parameter in the synthesis of ZnO-NPs, where reaction time is defined as the time necessary to completely reduce the metal ions. The results show that no absorption peak was found from 15 minutes to 1 hour (Fig. 2-b), yet once the reaction time reached 2 hours, the distinctive absorption peak was observed at 362 nm. This is consistent with prior research on *Catharanthus roseus* leaves, where the observation peak was likewise observed at 2 h (26), and on *C. roseus*, where observation peak was likewise observed at 2 h (27). The rise in absorbance intensity over time indicates that the nucleation and growth processes for ZnO-NPs have begun (28). The progressive variations in color of the combination were tracked by monitoring UV-visible absorption over time; this color shift was caused by the presence of bioactive chemicals in the *Z.-spina Christi* leaves extract. Zinc ion reduction is caused by a variety of phytochemicals. Since phenols and flavonoids contain a lot of OH groups, they function as stabilizers and bio-reducers of zinc compounds into zinc oxide nanoparticles (29).

Surprisingly, temperatures had a considerable influence on the synthesis of ZnO-NPs (Fig. 2-c), When the temperature was changed to 60°C, the typical absorption peak at 362 nm was detected. The higher the activation energy of the molecules, the faster the reaction rate, resulting in a decrease in the size of the nanoparticles and the formation of monodispersed smaller-sized

nanoparticles. The current study discovered that when temperature increases, the size of ZnO-NPs decreases, as evidenced by the sharp and thin surface plasmon resonance (SPR) peaks (30). UV-visible spectroscopy data from ZnO-NPs synthesized at various temperatures revealed peaks at 376 nm, 370 nm, 362 nm, and 348 nm for 40°C, 50°C, 60°C, 70°C respectively (Fig. 2-c).

The effect of pH on the synthesis of ZnO-NPs is significant. It was discovered that at pH 9.0, the characteristic absorption peak of ZnO-NPs was observed at 362 nm (Fig. 2-d), indicating that metal oxide reduction and zinc nitrate hexahydrate was converted to ZnO-NPs, whereas when the reaction medium was at alkaline condition that was more favorable to the synthesis of ZnO-NPs than acidic or neutral condition. The influence of pH (5.0-10.0) on the synthesis of ZnO-NPs using Aloe vera skin extract (31) discovered that the optimal pH required for the biosynthesis of ZnO-NPs was 8.0, which was similar to our results. As a result, ZnO-NPs were formed at pH 9.0 in the following experiments.

The FT-IR spectrum validated the production of ZnO-NPs by comparing the positions and intensities of peaks in *Z.-spina Christi* leaf extract to those generated in ZnO-NPs. The results demonstrated that the band locations and absorption intensities from the plant extract peak had changed, and that new peaks appeared in the FT-IR spectra of the produced ZnO-NPs. The observed spectra suggested that biological substances produced by *Z.-spina Christi* leaf extract were involved in the reduction and capping of ZnO-NPs. In this work, Zn<sup>2+</sup> is postulated to react with biological components found in *Z.-spina Christi* leaves extract, such as flavonoids, phenolic compounds, alkaloids, amino acids, tannins, and carbohydrates, to stimulate the production of ZnO-NPs and to act as a capping and stabilizing agent. Additionally, peaks at 451.34, 445.56, and 424.34 cm<sup>-1</sup> in the ZnO-NPs spectra match ZnO core bands that are

lacking in *Z.-spina Christi* leaf extract, verifying the nature of ZnO-NPs. This discovery was consistent with previous research, which found multiple Zn-O bands at 416.14, 515, and 618  $\text{cm}^{-1}$  (32,33). As a result, biological synthesis does not require any chemical sources for stabilizers, which is an advantage over chemical synthesis.

As an X-ray passes through a particle crystal, a diffraction pattern is formed, which gives information on the atomic arrangement within the crystals. The peaks in the XRD diffractogram (Fig. 4) appeared to be broadening, revealing that perhaps the ZnO-NPs were formed on the nanoscale. When compared with the Joint Committee on Powder Diffraction Standards (JCPDS) Card No. 36-1451, the most intense diffraction peaks found were indexed as the hexagonal wurtzite structure of ZnO-NPs with high crystallinity, as illustrated in Figure 4. All of the distinctive peaks were found to be ZnO-NPs, and no such impurities were found in produced ZnO-NPs. These findings were consistent with earlier researches (34,35).

The TEM method was used to examine the biosynthesized ZnO-NPs. The acquired micrographs show that the biosynthesized ZnO-NPs were agglomerated particles that were spherical and hexagonal in shape, with an average particle size of 43.35 nm. The existence of halo rings shows that these particles are amorphous in certain areas. The existence of spherical particles is attributed to an amorphous phase with no crystallographic orientation. ZnO-NPs are capped by hexagonal molecules and biomolecules. Similar hexagonal molecules have been found in ZnO-NPs synthesis in *Euphorbia jatropha* plants (36). Figures exhibit TEM pictures of the synthesized ZnO-NPs that are nano-crystalline (Fig. 5-a, b). The biomolecules found in *Z.-Spina Christi* leaf extract influenced the formation of ZnO ZnO-NPs. These findings are consistent with earlier publications (37,38).

In vivo studies on the effects of ZnO-NPs and *Z.-Spina Christi* leaf extract on rats with adenine-induced chronic kidney disease (CKD). Our findings suggest that administering ZnO-NPs and *Z.-Spina Christi* leaf extract to healthy male rats is not entirely risk-free. The adenine induced renal failure model provides significant

information regarding the route mechanism of different renal shortage problems. When compared to renal failure issues in people, it created metabolic exceptions in male rats, and it is used as a disease model to measure therapeutic action(39).

The initial impact of ZnO-NPs on male rats in renal failure caused by adenine was examined in this work. Adenine administration to rats resulted in body weight loss due to the buildup of uremic toxins, which causes inflammation and activation of protein catabolic pathways, resulting in protein breakdown (40). Rats after 30 days of treatment with ZnO-NPs at concentrations of (10 mg/kg BW) showed a slight decrease in body weight; the decreases may be due to ZnO-NPs at this dose causing instability in protein degradation and lipid metabolism, resulting in an increase or decrease in body weight (41), depending on the effect of dose and treatment period. Moreover, ZnO-NPs may accumulate in numerous animal organs such as the kidney and liver, causing alterations in tissue functioning and, as a result, altering metabolic rate. Another study found that giving rats ZnO-NPs at different dosages (5, 50, and 100 mg/kg.BW) for 14 days resulted in a considerable reduction in body weight (42). In addition, research conducted by (43) on Wistar rats treated with ZnO-NPs at a concentration of (10 mg/kg.BW) revealed a non-significant influence on body weight increase, indicating the absence of hazardous indicators and mortality in adult male rats exposed to ZnO-NPs. Table 1 shows that there was a less significant change in weights in all rats after treatment with aqueous leaf extract of *Z. spina-Christi* at a level of (10 mg/kg.BW). The weight loss in these rats might be attributed to anti-nutritional bioactive components in the plant extract, such as tannin, flavonoids and phenolic compounds (44).

When compared to the control group, there was an increase in blood levels of uric acid, urea, and creatinine in the second group rats (G-II). These findings were characterized by renal dysfunction, as evidenced by congestion and necrosis of the renal glomeruli, as well as degenerative changes and necrosis of the normal renal tubular epithelium lining renal tubules (45), because of these products accumulate in the bloodstream

and formation of 2,8-dihydroxyadenine crystals, result in high accumulation of different guanidino compounds such as (gaunidinosuric acid and methyl-guanidine) and nitrogenous compounds with renal failure (46). Administration of ZnO-NPs (10 mg/kg B.W) to rats in third group (G-III) showed that significant differences ( $P < 0.05$ ) were observed in the levels of uric acid, urea, and creatinine in comparison to the control group, whereas administration of Z.-Spina Christi leaves extract (10 mg/kg B.W) to rats in fourth group (G-IV) revealed a less significant difference in the levels of uric acid, urea, and creatinine in comparison to the control group ( $P < 0.05$ ), this indicates that dosage of Z.-Spina Christi leaves extract (10 mg/kg B.W) has no negative effect on the kidneys. However, serum levels of uric acid, urea, and creatinine showed a significant decrease ( $P < 0.05$ ) after the administration of adenine plus ZnO-NPs (10 mg/kg B.W) or adenine plus Z.-Spina Christi leaves extract ZnO-NPs (10 mg/kg B.W) at the same time in both fifth and sixth groups rats (G-V and G-VI) by comparison to adenine group and a significant increase ( $P < 0.03$ ) with comparison to control rats, which evaluated that the synthesized ZnO-NPs and Z.-Spina Christi leaves might be able to avoid the damaged renal excretion, i.e., kidney alterations with adenine-induced renal failure. These results are in agreement with previous study (47).

found that adenine impaired antioxidant enzyme activity and significantly increased oxidative stress indicators in kidney tissue. Furthermore, as shown in table 3, the anti-inflammatory activities of ZnO-NPs and Z.-Spina Christi leaves extract are corroborated by a considerable rise in TAC and CAT levels linked with a decrease in MDA concentration. Z.-Spina Christi leaves extract and ZnO-NPs were able to significantly decrease renal failure induced by adenine, but observed that the co-administration of adenine plus Z.-Spina Christi leaves extract (10 mg/kg B.W) (G-VI) gave better results when compared to the adenine plus ZnO-NPs (10 mg/kg B.W) (G-V), noted that aqueous leaf extract of Z.-Spina Christi improved adenine-induced oxidative injury on the kidney by its antioxidant and free radical-scavenging properties. These results were

harmonic with the previous record of (40) who suggested that the main mechanism for the beneficial action of gum acacia in adenine-induced kidney disease via its antioxidant properties. Furthermore, the kidney was protected by the aqueous extract of Z.-Spina Christi leaves against adenine-induced toxicity due to its important contents of flavonoids, phenolic compounds, saponins and triterpenes (48).

The results of the histological investigation matched those of the biochemical analysis. The histological analysis found that adenine caused stripping of the renal tubule epithelium due to its metabolite, DHA(2-8 dihydroxy adenine), which has low solubility and can precipitate in the renal tubules leading to their obstruction and development of uremia with exudate of inflammatory cells and glomeruli, significant dilation and necrosis of renal tubules as showed in (Fig. 6-K2) (49), this also due to that adenine increase creatinine and urea in plasma, and is capable of oxidative stress in renal tissue causing histological damage in the kidneys (50). The kidney of group rats when treated with the adenine plus ZnO-NPs (10 mg/kg B.W) or adenine plus Z.-Spina Christi leaves extract (10 mg/kg B.W) (Fig. 6-K5 and K6) showed improvement the glomerular to normal renal tubules and normal histological appearance. These findings are consistent with previous plant research (51), these results show the synthesized ZnO-NPs and Z.-Spina Christi leaves extract protected the normal glomeruli and avoided damage as well as a little epithelial extended and mononuclear cell infiltration (52). According to pathological changes in renal tissue (fig. 6-K5 and K6), the combined therapy for ZnO-NPs and Z.-Spina Christi leaves in their oral administrations possible that consider a defensive role to avoid damage of tubular and glomerular (53). The activity of reproductive epithelial cells in the renal tissues enhanced greatly following treatment with Z.-Spina Christi leaf extract. The antioxidant, anti-inflammatory, and analgesic properties of Z.-Spina Christi leaves extract can be attributed to the presence of some active biological components, flavonoids, and phenolic compounds that have the ability to scavenge free

radicals and active oxygen species such as singlet oxygen, free radicals, and hydroxyl radicals (54).

### CONCLUSION

The biogenesis of zinc oxide nanoparticles was obtained in this study by employing *Z. spina Christi* leaf extract as a reducing and capping agent. UV-visible, FTIR, XRD, and TEM studies were used to characterize ZnO-NPs. Our findings show that synthesized ZnO-NPs and aqueous leaf extract of *Z. spina Christi* at (10 mg/kg B.W) respectively, have protective effects against renal failure induced by adenine in male rats, implying that they may be used safely against kidney damage at this concentration; no significant effects were observed in normal renal tissues, implying that they may be powerful antioxidant, anti-inflammatory, and antitoxic agents for commercial biomedical applications.

### REFERENCES

1. Santilli CV, Tokumoto MS, Briois V, Santilli C v, Pulcinelli SH. Preparation of ZnO nanoparticles: Structural study of the molecular precursor Cite this paper Preparation of ZnO Nanoparticles: Structural Study of the Molecular Precursor. Vol. 26, Journal of Sol-Gel Science and Technology. 2003.
2. Becheri A, Dürr M, lo Nostro P, Baglioni P. Synthesis and characterization of zinc oxide nanoparticles: Application to textiles as UV-absorbers. Journal of Nanoparticle Research. 2008 Apr;10(4):679–89.
3. Jahn W. Review: Chemical Aspects of the Use of Gold Clusters in Structural Biology [Internet]. 1999. Available from: <http://www.ideallibrary.com>
4. Shah RK, Boruah F, Parween N. Synthesis and characterization of ZnO nanoparticles using leaf extract of *Camellia sinesis* and evaluation of their antimicrobial efficacy. Int J Curr Microbiol App Sci. 2015;4(8):444–50.
5. Morkoç H, Özgür Ü. Zinc oxide: fundamentals, materials and device technology. John Wiley & Sons; 2008.
6. Özgür Ü, Alivov YI, Liu C, Teke A, Reshchikov MA, Doğan S, et al. A comprehensive review of ZnO materials and devices. Vol. 98, Journal of Applied Physics. 2005. p. 1–103.
7. Shamsuzzaman AA, Asif M, Mashrai A, Khanam H. Green Synthesis of ZnO Nanoparticles Using *Bacillus Subtilis* And Their Catalytic Performance In The One-Pot Synthesis of Steroidal Thiophenes. European Chemical Bulletin. 2014;3(9):939–45.
8. Mohamed HYG, Ismael E, Elaasser MM, Khalil MMH. Green synthesis of zinc oxide nanoparticles using portulaca oleracea (regla seeds) extract and its biomedical applications. Egypt J Chem. 2021;64(2):661–72.
9. Kang T, Guan R, Chen X, Song Y, Jiang H, Zhao J. In vitro toxicity of different-sized ZnO nanoparticles in Caco-2 cells. Nanoscale Res Lett. 2013;8(1):1–8.
10. Rasmussen JW, Martinez E, Louka P, Wingett DG. Zinc Oxide Nanoparticles for Selective Destruction of Tumor Cells and Potential for Drug Delivery Applications.
11. Loh AH, Cohen AH. Drug-induced kidney disease-pathology and current concepts. Ann Acad Med Singapore. 2009;38(3):240–50.
12. Alqatab AH, Hassan AH. Evaluation of some Coagulation Factors in Male rat with Induce Chronic Renal Failure (CRD). Res J Pharm Technol. 2019;12(4):1871–4.
13. Cullity BD. Elements of X-ray Diffraction, Adison–Wesley Publ. Co, London. 1967;
14. Health NI of. Guide for the care and use of laboratory animals. National Academies; 1985.
15. al Za'abi M, al Busaidi M, Yasin J, Schupp N, Nemmar A, Ali BH. Development of a new model for the induction of chronic kidney disease via intraperitoneal adenine administration, and the effect of treatment with gum acacia thereon. Am J Transl Res. 2015;7(1):28.
16. Yokozawa T, Zheng PD, Oura H, Koizumi F. Animal model of adenine-induced chronic renal failure in rats. Nephron. 1986;44(3):230–4.
17. Awadalla A, Hamam ET, El-Senduny FF, Omar NM, Mahdi MR, Barakat N, et al. Zinc oxide nanoparticles and spironolactone-enhanced Nrf2/HO-1 pathway and inhibited Wnt/ $\beta$ -catenin pathway in adenine-induced nephrotoxicity in rats. Redox Report. 2022;27(1):249–58.
18. Bashandy SAE, Ahmed-Farid OAH, Abdelmottaleb-Moussa S, Omara EA, Abdel Jaleel GA, Ibrahim FAA. Efficacy of zinc oxide nanoparticles on hepatocellular carcinoma-induced biochemical and trace element alterations in rats. J Appl Pharm Sci. 2021;11:108–17.
19. Alzahrani F, Al-Shaebi EM, Dkhil MA, Al-Quraishy S. In vivo anti-eimeria and in vitro anthelmintic activity of *Ziziphus spina-christi* leaf extracts. Pak J Zool. 2016;48(2).
20. Bashandy SAE, Alaamer A, Moussa SAA, Omara EA. Role of zinc oxide nanoparticles in alleviating hepatic fibrosis and nephrotoxicity induced by thioacetamide in rats. Can J Physiol Pharmacol. 2018;96(4):337–44.
21. Ji X, Zhang F, Zhang R, Liu F, Peng Q, Wang M. An acidic polysaccharide from *Ziziphus Jujuba*

- cv. Muzao: Purification and structural characterization. *Food Chem.* 2019;274:494–9.
22. Cun T, Dong C, Huang Q. Ionothermal precipitation of highly dispersive ZnO nanoparticles with improved photocatalytic performance. *Appl Surf Sci.* 2016;384:73–82.
  23. Ramimoghadam D, Hussein MZ bin, Taufiq-Yap YH. The effect of sodium dodecyl sulfate (SDS) and cetyltrimethylammonium bromide (CTAB) on the properties of ZnO synthesized by hydrothermal method. *Int J Mol Sci.* 2012;13(10):13275–93.
  24. Wang Q, Mei S, Manivel P, Ma H, Chen X. Zinc oxide nanoparticles synthesized using coffee leaf extract assisted with ultrasound as nanocarriers for mangiferin. *Curr Res Food Sci.* 2022;
  25. Król A, Pomastowski P, Rafińska K, Railean-Plugaru V, Buszewski B. Zinc oxide nanoparticles: Synthesis, antiseptic activity and toxicity mechanism. *Adv Colloid Interface Sci.* 2017;249:37–52.
  26. Gupta M, Tomar RS, Kaushik S, Mishra RK, Sharma D. Effective antimicrobial activity of green ZnO nano particles of *Catharanthus roseus*. *Front Microbiol.* 2018;9:2030.
  27. Kalaiselvi A, Roopan SM, Madhumitha G, Ramalingam C, Al-Dhabi NA, Arasu MV. *Catharanthus roseus*-mediated zinc oxide nanoparticles against photocatalytic application of phenol red under UV@ 365 nm. *Curr Sci.* 2016;1811–5.
  28. Goh EG, Xu X, McCormick PG. Effect of particle size on the UV absorbance of zinc oxide nanoparticles. *Scr Mater.* 2014;78:49–52.
  29. Singh P, Kim YJ, Zhang D, Yang DC. Biological Synthesis of Nanoparticles from Plants and Microorganisms. Vol. 34, Trends in Biotechnology. Elsevier Ltd; 2016. p. 588–99.
  30. al Awadh AA, Shet AR, Patil LR, Shaikh IA, Alshahrani MM, Nadaf R, et al. Sustainable synthesis and characterization of zinc oxide nanoparticles using *Raphanus sativus* extract and its biomedical applications. *Crystals (Basel).* 2022;12(8):1142.
  31. Ali K, Dwivedi S, Azam A, Saquib Q, Al-Said MS, Alkhedhairy AA, et al. Aloe vera extract functionalized zinc oxide nanoparticles as nanoantibiotics against multi-drug resistant clinical bacterial isolates. *J Colloid Interface Sci.* 2016;472:145–56.
  32. Dobrucka R, Długaszewska J. Biosynthesis and antibacterial activity of ZnO nanoparticles using *Trifolium pratense* flower extract. *Saudi J Biol Sci.* 2016;23(4):517–23.
  33. Ebadi M, Zolfaghari MR, Aghaei SS, Zargar M, Shafiei M, Zahir HS, et al. A bio-inspired strategy for the synthesis of zinc oxide nanoparticles (ZnO NPs) using the cell extract of cyanobacterium *Nostoc* sp. EA03: from biological function to toxicity evaluation. *RSC Adv.* 2019;9(41):23508–25.
  34. Jayachandran A, Aswathy TR, Nair AS. Green synthesis and characterization of zinc oxide nanoparticles using *Cayratia pedata* leaf extract. *Biochem Biophys Rep.* 2021;26:100995.
  35. Dey A, Somaiah S. Green synthesis and characterization of zinc oxide nanoparticles using leaf extract of *Thryallis glauca* (Cav.) Kuntze and their role as antioxidant and antibacterial. *Microsc Res Tech.* 2022;
  36. Geetha MS, Nagabhushana H, Shivananjaiah HN. Green mediated synthesis and characterization of ZnO nanoparticles using *Euphorbia Jatropha latex* as reducing agent. *Journal of Science: Advanced Materials and Devices.* 2016;1(3):301–10.
  37. Suresh J, Pradheesh G, Alexramani V, Sundrarajan M, Hong SI. Green synthesis and characterization of zinc oxide nanoparticle using insulin plant (*Costus pictus* D. Don) and investigation of its antimicrobial as well as anticancer activities. *Advances in Natural Sciences: Nanoscience and Nanotechnology.* 2018;9(1):015008.
  38. Pillai AM, Sivasankarapillai VS, Rahdar A, Joseph J, Sadeghfard F, Rajesh K, et al. Green synthesis and characterization of zinc oxide nanoparticles with antibacterial and antifungal activity. *J Mol Struct.* 2020;1211:128107.
  39. Törmänen S, Pörsti I, Lakkisto P, Tikkanen I, Niemelä O, Paavonen T, et al. Endothelin A receptor blocker and calcimimetic in the adenine rat model of chronic renal insufficiency. *BMC Nephrol.* 2017;18(1):1–13.
  40. al Za'abi M, al Busaidi M, Yasin J, Schupp N, Nemmar A, Ali BH. Development of a new model for the induction of chronic kidney disease via intraperitoneal adenine administration, and the effect of treatment with gum acacia thereon. *Am J Transl Res.* 2015;7(1):28.
  41. Shirvani H, Noori A, Mashayekh AM. The effect of ZnO nanoparticles on the growth and puberty of newborn male Wistar rats. *International Journal of Basic Sciences & Applied Research.* 2014;3:180–5.
  42. Mansouri E, Khorsandi L, Orazizadeh M, Jozi Z. Dose-dependent hepatotoxicity effects of zinc oxide nanoparticles. 2015;
  43. Ben SI. Sub-acute oral toxicity of zinc oxide nanoparticles in male rats. 2015;
  44. Alebachew M, Kinfu Y, Makonnen E, Bekuretsion Y, Urga K, Afework M. Toxicological evaluation of methanol leaves extract of *Vernonia bipontini* Vatke in blood, liver and kidney tissues of mice. *Afr Health Sci.* 2014;14(4):1012–24.
  45. Mehrdad M, Mozghan GP. Effect of Zingiber Extract on Histopathologic Changes in Mice Kidneys. *Res J Appl Sci.* 2011;6(5):1–3.

46. ali Imarah A, AL-Ghurabi ME. Induction of Acute Renal Failure to Study of Some Physiological and Histological Criteria in Rats Before and After Treatment with Eruca Sativa Oil Extract of Leaves. *Journal of Pharmaceutical Sciences and Research*. 2017;9(7):1045.
47. Cai H, Su S, Li Y, Zeng H, Zhu Z, Guo J, et al. Protective effects of *Salvia miltiorrhiza* on adenine-induced chronic renal failure by regulating the metabolic profiling and modulating the NADPH oxidase/ROS/ERK and TGF- $\beta$ /Smad signaling pathways. *J Ethnopharmacol*. 2018;212:153–65.
48. Khaleel SM, Almuhr RA, Al-Deeb TMF, Jaran AS. Biochemical changes in the liver, kidney and serum of rats exposed to ethanolic leaf extract of *Ziziphus spina-christi*. *Jordan J Biol Sci*. 2021;14(4).
49. Engle SJ, Stockelman MG, Chen JU, Boivin G, Yum MN, Davies PM, et al. Adenine phosphoribosyltransferase-deficient mice develop 2, 8-dihydroxyadenine nephrolithiasis. *Proceedings of the National Academy of Sciences*. 1996;93(11):5307–12.
50. Pettitt RM, Brumbaugh AP, Gartman MF, Jackson AM. Chronic kidney disease: Detection and evaluation. *Osteopathic Family Physician*. 2020;12(1):14–9.
51. Singh D, Chopra K. The effect of naringin, a bioflavonoid on ischemia-reperfusion induced renal injury in rats. *Pharmacol Res*. 2004;50(2):187–93.
52. Abd El-Megeid AA, AbdAllah IZA, Elsadek MF, Abd El-Moneim YF. The protective effect of the fortified bread with green tea against chronic renal failure induced by excessive dietary arginine in male albino rats. *World Journal of Dairy & Food Sciences*. 2009;4(2):107–17.
53. Sayhan MB, Kanter M, Oguz S, Erbogaa M. Protective effect of *Urtica dioica* L. on renal ischemia/reperfusion injury in rat. *J Mol Histol*. 2012;43(6):691–8.
54. Schulman G, Agarwal R, Acharya M, Berl T, Blumenthal S, Kopyt N. A multicenter, randomized, double-blind, placebo-controlled, dose-ranging study of AST-120 (Kremezin) in patients with moderate to severe CKD. *American journal of kidney diseases*. 2006;47(4):565–77.